Fall 9-29-2014

Carboxymethylcellulose hydrogels support central nervous system-derived tumor-cell chemotactic migration: comparison with conventional extracellular matrix macromolecules

Tanya Singh
CUNY City College

Chandrasekhar Kothapalli
Cleveland State University

Devika Varma
CUNY City College

Steven B. Nicoll
CUNY City College

Maribel Vazquez
CUNY City College

Article

JOURNAL OF
biomaterials
applications

Journal of Biomaterials Applications
2014, Vol. 29(3) 433–441

DOI: 10.1177/0885328214532969
jba.sagepub.com
SAGE

Carboxymethylcellulose hydrogels support central nervous system-derived tumor-cell chemotactic migration: Comparison with conventional extracellular matrix macromolecules

Tanya Singh[1], Chandrasekhar Kothapalli[2], Devika Varma[1], Steven B Nicoll[1] and Maribel Vazquez[1]

Abstract

The local microenvironment plays an important role in maintaining the dynamics of the extracellular matrix and the cell–extracellular matrix relationship. The extracellular matrix is a complex network of macromolecules with distinct mechanical and biochemical characteristics. Disruptions in extracellular matrix homeostasis are associated with the onset of cancer. The extracellular matrix becomes highly disorganized, and the cell–matrix relationship changes, resulting in altered cell-signaling processes and metastasis. Medulloblastoma is one of the most common malignant pediatric brain tumors in the United States. In order to gain a better understanding of the interplay between cell–extracellular matrix interactions and cell-migratory responses in tumors, eight different matrix macromolecule formulations were investigated using a medulloblastoma-derived cell line: poly-D-lysine, matrigel, laminin, collagen 1, fibronectin, a 10% blend of laminin–collagen 1, a 20% blend of laminin–collagen 1, and a cellulose-derived hydrogel, carboxymethylcellulose. Over time, the average changes in cell morphology were quantified in 2D and 3D, as was migration in the presence and absence of the chemoattractant, epidermal growth factor. Data revealed that carboxymethylcellulose allowed for a cell–extracellular matrix relationship typically believed to be present in tumors, with cells exhibiting a rounded, amoeboid morphology consistent with chemotactic migration, while the other matrices promoted an elongated cell shape as well as both haptotactic and chemotactic motile processes. Therefore, carboxymethylcellulose hydrogels may serve as effective platforms for investigating central nervous system-derived tumor-cell migration in response to soluble factors.

Keywords

Medulloblastoma, carboxymethylcellulose, chemotaxis, migration, macromolecules

Introduction

The matrix microenvironment plays a critical role in cell migration, as cells are well known to interact with the proteins of the surrounding extracellular matrix (ECM) to achieve locomotion (reviewed in Berrier and Yamada,[1] Lu et al.,[2] and Zaman et al.[3]). The ECM chosen for cancer study is particularly important because the ECM of the tumor environment is known to have lower protein density,[1] higher matrix stiffness,[1,2,4] increased hydrophobicity,[5] and increased cytokine and growth factor concentrations than physiological ECM, primarily as a result of tumor hypervascularity.[2,6–8] Furthermore, cell–ECM dynamics change during tumor progression, as the surrounding matrix now facilitates cellular de-differentiation and becomes more porous and "leaky"[9,10] to enable metastasis, immune-cell infiltration, and cancer-cell progression.[11,12] Such

[1]Department of Biomedical Engineering, The City College of New York-CUNY, USA
[2]Department of Chemical and Biomedical Engineering, Cleveland State University, USA

Corresponding author:
Maribel Vazquez, 160 Convent Avenue, Steinman Hall 403D, New York, NY 10031, USA.
Email: vazquez@me.ccny.cuny.edu

ECM changes are particularly acute in tumors of the central nervous system (CNS), as ECM within brain varies greatly across anatomical regions[13] between healthy and injured brain and amid CNS tissue with different types and grades of neural tumors (reviewed in Richard et al.[14]). As a result, the migration of cells derived from CNS tumors has been extensively studied in both 2D[1,3,15] and 3D ECM models[16–18] using constituent proteins of ECM found inside and outside of the CNS. These include collagen type I (C-1),[1,15,19] fibrin,[3,8] fibronectin (FN),[1,3] laminin (LN),[20,21] matrigel (MGL), hyaluronan, chitosan,[8] and numerous blends thereof. In addition, several researchers have explored a variety of synthetic and natural materials as ECM substitutes for clinical and surgical use[22–27] within the CNS, such as polyacrylamide,[28] poly(ethylene glycol), poly(*N*-isopropylacrylamide), poly-L-lysine, methylcellulose, poly(lactic acid), and pluronic F127 (an ABA block copolymer made up of poly(propylene oxide) and poly(ethylene oxide)).[8] These hydrogels have been shown to provide several advantages in cancer treatment because they are minimally invasive,[29] highly localized, and can reduce cell aggregation.[8]

As the ECM of the CNS is well known to change properties during tumorigenesis[2,11,12,21,30] and dissemination,[14,31–33] the goal of this study is to identify an ECM material with minimal cell-integrin interactions so as to enable more controlled study of migration patterns and motility of brain cancer cells to chemical microenvironments (i.e. controlled chemotaxis[1,14,34,35]). This is of high significance because anti-migratory pharmaceuticals are not currently investigated as potential chemotherapies for CNS patients since pharmacologically induced chemotaxis is particularly affected by ECM-dependent cellular responses in the brain.[36,37]

In this work, we examine carboxymethylcellulose (CMC) as a so-called haptotaxis-neutral biomaterial to function as an ECM macromolecule for CNS tumor-cell chemotaxis. CMC is a biocompatible, cellulose-derived hydrogel composed of a polysaccharide backbone with periodic side chains of carboxymethyl groups. CMC has recently been shown to support nucleus pulposus-cell viability and phenotypic matrix deposition and to promote mesenchymal stem-cell chondrogenesis and functional matrix assembly *in vitro*.[38,39] Here, the effect of CMC on the morphology and migration of CNS-derived tumor cells was compared with eight ECM macromolecules. Specifically, this study investigated tumor-cell responses within (i) MGL, a commercial matrix material most commonly used to mimic brain; (ii) poly-D-lysine (PDL), the polymer used to coat tissue-culture substrates; (iii) collagen-1 (C-1), the major fibrous protein in mammalian ECM; (iv) laminin (LN), a primary protein found in the brain; (v) FN, a principal component of brain tumor ECM not readily present in healthy CNS; (vi) a blend of C-1 and 10% LN (CL10) (v/v) newly used for *in vitro* motility experiments of neurons;[8] (vii) a blend of C-1 and 20% LN (CL20) (v/v); and (viii) CMC, a plant-derived polysaccharide previously unused in CNS research. The results illustrate that the cells were indeed able to migrate within the CMC and survive for up to 6 days. Furthermore, CMC induced integrin expression in a pattern similar to that seen with CNS cells upon LN. This study is among the first to identify the CMC hydrogel as a novel biomaterial for testing of anti-migratory therapeutics for tumors of the CNS.

Materials and methods

Cell culture

Medulloblastoma (MB)-derived Daoy-cell line (ATCC cat no. HTB-186, Manassas, VA) was established from a tumor biopsy of a 4-year-old boy. Daoy cells were thawed, plated, and cultured in sterile Eagle minimum essential medium (EMEM) containing 9% fetal bovine serum ((Mediatech Inc., Manassas, VA), 2% L-glutamine (Mediatech Inc.), and 1% penicillin–streptomycin (Mediatech Inc.) as done previously in our laboratory.[40] Cells were cultured (37°C, 95% humidity, 5% CO_2) and passaged (<70% confluency) on sterile plasma-treated polystyrene tissue-culture flasks (BD Biosciences, Franklin Lakes, NJ) until further use.

Preparation of 2D and 3D substrates for cell culture

Solutions for 2D substrates were prepared as follows: PDL (Sigma-Aldrich, St, Louis, MO) solution was prepared in sterile phosphate-buffered saline (1 × PBS) at 100 μg/mL final concentration, added to two-well Nunc Lab-Tek II chamber slides (Thermo Fisher Scientific, Waltham, MA) to coat overnight at room temperature, washed with PBS (Sigma), and dried. FN (Sigma) was diluted in PBS to 0.005% (v/v) concentration and coated on two-well slides as described above. Growth factor-reduced MGL (BD Biosciences cat # 356230) was thawed at 4°C overnight and reconstituted at 100 μg/mL final concentration in sterile ice-cold PBS. Two-chamber slides were coated with this solution for 1 h at room temperature and immediately seeded with cells. C-1 solution (rat tail-derived, 8.61 mg/mL; BD Biosciences cat no. 354249, Bedford, MA) was prepared to a final concentration of 50 μg/mL (pH 7.4). C-1 was added to two-well slides, incubated at 37°C for 1 h, washed with PBS, and stored at 4°C. Similarly, slides were coated with collagen–LN

(10% or 20%, v/v) solutions, prepared by combining C-1 solution (50 μg/mL) with LN (BD Biosciences, cat no. 354239, 1 mg/mL), so that the final mixture contained either 10% or 20% (v/v) LN (CL10 or CL20, respectively). Daoy cells were seeded on these substrates at a density of 1×10^4 cells/well (n = 3 wells/case) and cultured for 3 days in EMEM medium. Controls (CTRL) consisted of Daoy cells seeded onto uncoated tissue-culture polystyrene.

Five different types of 3D hydrogel solutions were prepared. C-1 solution was reconstituted at 2 mg/mL (pH ~7.4) final concentration as detailed above. MGL was reconstituted in ice-cold PBS at 2 mg/mL concentration. CL10 and CL20 gels were prepared by mixing 2 mg/mL C-1 solution with 1 mg/mL LN, so that the final concentration of LN was either 10% or 20% (v/v). All the above solutions were maintained on ice until cell seeding. Daoy cells mixed in these solutions at a final concentration of 1:30 (cell:gel ratio) were seeded within two-chamber slides and allowed to polymerize at 37°C for 30 min in humidified chambers. EMEM medium was added to these chamber slides, and cultures maintained for 3 days with media changed after every 24 h.

Methacrylated CMC was synthesized through esterification of hydroxyl groups based on previous protocols.[49,50] Briefly, a 20-fold excess of methacrylic anhydride (Sigma, St. Louis, MO) was reacted with a 1 wt% solution of 250-kDa CMC (Sigma) in RNAse/DNAse-free water over 24 h at 4°C at a pH of 8.0. The methacrylated CMC solution was purified via dialysis for 96 h against RNAse/DNAse-free water to remove excess, unreacted methacrylic anhydride.

The purified methacrylated CMC was recovered by lyophilization and stored at –20°C. The degree of methacrylation (7.7%) was confirmed by ^{1}H-NMR. Lyophilized methacrylated CMC was sterilized by a germicidal UV light exposure for 30 min before dissolving it in filter-sterilized 0.05% photoinitiator, 2-methyl-1-[4-(hydroxyethoxy)phenyl]-2-methyl-1-propanone (Irgacure 2959, I2959; Ciba Specialty Chemicals, Basel, Switzerland), in sterile Dulbecco's PBS (DPBS) at 4°C to obtain a 2% (w/v) solution. The solution was gelled between two glass slides exposed to long-wave UV light (EIKO, Shawnee, KS; peak 368 nm, 1.2 W) for 10 min to produce covalently crosslinked hydrogel films. An 8-mm diameter stainless steel punch was used to obtain thin hydrogel discs with a thickness of ~550 μm.

Cell-morphology imaging and analysis

A Nikon TE2000 epi-fluorescence, inverted microscope equipped with short- and long-range objectives and a cooled CCD camera (CoolSNAP EZ, Photometrics, Tucson, AZ) was used for imaging cells. Images were obtained in both phase-contrast and fluorescence modes (for stained cultures, n = 5) to verify the cell attachment and unchanged morphology for up to 7 days. However, only data for 3 days were shown in order to provide quantitative metrics for the fluorescence dye (CellTracker^{TM}). Images were analyzed using the National Institutes of Health (NIH) ImageJ software. The projected area (A) and perimeter (P) for each cell were measured under the defined culture conditions, and the average cell morphology was analyzed using the cell shape index ($CSI = 4\pi A/P^2$), as reported previously by our group and others.[41,42] The cell count varied between 15 and 50 cells for each culture condition to determine the respective CSI.

Transwell assay for cell migration

Transwells of 8-μm pore size (polycarbonate membranes, 10-μm thickness, tissue-culture treated; VWR, cat no. 62406-198) were used to measure cell migration through 3D matrix molecules. Thirty microliters of each gel was loaded into the inserts (n = 6/case) and allowed to polymerize (37°C, 30 min, 95% humidity). The final gel thickness in each well was ~0.38 mm. The inserts were placed within individual wells in a 24-well plate and 20 μL of Daoy-cell solution (1×10^4 cells/mL). Complete medium was added to the wells as well as the inserts to prevent gels from drying and incubated at 37°C with 5% CO_2 for 48 h. Cell migration across the gel and transwell was measured at two different time points of $t_1 = 24$ h and $t_2 = 48$ h (n = 3 wells/time point). Excess medium was aspirated, and the non-motile cells were removed from the upper surface of the membrane by quickly cleaning the hydrogel surface. Inserts were then rinsed in sterile PBS and stained using the Diff-Quik staining kit (Allegiance) as per the recommended protocols. Cell counting was performed via hemocytometer as done previously in our laboratory[43] by measuring cells within images of the membrane obtained at low magnification using a Nikon TE2000 inverted microscope.

MTT cell-proliferation assay

The Vybrant MTT Cell Proliferation Assay Kit (Invitrogen Molecular Probes, cat no. V-13154, Eugene, OR) was used to determine the cell viability. The MTT kit reagents were prepared according to the provided protocol. CMC hydrogels were prepared and placed in Boyden chambers in a 24-well plate, which were then seeded with Daoy cells that were stimulated with 1000 ng/mL of epidermal growth factor (EGF), previously shown to be a chemoattractant for these cells.[40,41] For labeling the cells, old media from the

Boyden chambers were removed and replaced with 100 μL of fresh complete culture medium.

Samples were treated with 10 μL of the 12 mM MTT stock solution and incubated for 2–4 h. After incubation, samples were treated with 100 μL of the SDS–HCl solution and incubated for 4–18 h, and the absorbance was then read at 570 nm in a 96-well plate. To correct for background absorbance, measurements from culture medium-containing MTT and SDS–HCl solutions were subtracted from those for the experimental samples. Analysis was performed at three time points (24, 48, and 72 h), and each experiment was done in triplicate. CTRL consisted of Daoy cells seeded on tissue-culture polystyrene.

Spectro analysis

A Zeiss Axio Observer inverted microscope was used to compile digital sections (i.e. z-stacks) of the CMC hydrogels seeded with cells in a 24-well plate after 72 h. Prior to seeding, the cells were stained with a cell membrane dye, CellTracker™ Green CMFDA (Invitrogen), for 45 min in a 15 μM dye solution followed by a 30-min incubation step in pre-warmed complete DMEM medium. Only data for 3 days were shown in order to provide quantitative metrics for CellTracker.

Various positions on the hydrogel were selected. Slices of images were captured for each position at 5.44 -μm intervals through the depth of the hydrogel. The number of images obtained depended on the height of the z-stack analysis. Representative serial sections were used to display cells on different focal planes within the gel.

Immunocytochemistry (ICC) staining

Samples were prepared in a four-well confocal plate with coatings of either C-1 (2 mg/mL) LN (1 mg/mL), MGL (100 mg/mL), or CMC (2% w/v). CTRL cells were plated directly onto confocal plates. Cells were seeded at a density of 5000 cells in 500 μL and incubated on substrates for ~2 h. The culture medium was then aspirated, and the samples were rinsed with PBS and fixed with 2–4% formalin for 10 min. Prior to staining, specimens were rinsed, permeabilized with 0.1% Triton-X in PBS for 10 min, and incubated for 60 min in 1% blocking solution (PBSA). After incubation, the samples were washed with 1% PBS–BSA solution, exposed to 5 μg/mL of $\alpha_v\beta_3$ antibody (Millipore, MAB1976X, Billerica, MA), and incubated overnight at 4°C. The samples were then washed with PBS and incubated in Hoechst 33342 nuclear dye for 25 min.

Confocal imaging via Zeiss LSM 710 microscope was utilized to visualize the integrin expression by cells seeded on each matrix. Integrin expression was quantified by measuring the staining intensity of individual cells using NIH-approved Image J software. The mean integrin expression was obtained for a sample group of n = 4 for C-1, LN, MGL, and CMC.

Statistical analysis

One-way analysis of variance (ANOVA) was performed using Origin (version 7.5) followed by Tukey comparison to identify statistically significant interactions between groups. Each experiment was performed between three and five times by different co-authors. Significance level was set to $p < 0.05$.

Results

The different biopolymers used as ECM macromolecules for this study were chosen based on their reported abilities to promote cell attachment, growth, and migration.

The changes in average CSI of MB-derived Daoy cells plated on 2D substrates from day 1 to day 3 are shown in Figure 1. The values of CSI for cells adherent to 2D substrates of ECM macromolecules comprised of C-1 (0.54 ± 0.026), LN (0.62 ± 0.04), PDL (0.67 ± 0.02), FN (0.63 ± 0.027), and MGL (0.67 ± 0.04) were not significantly different from one another and averaged 0.62 ± 0.05 over the 3-day time period. By contrast, much larger changes in cell shape

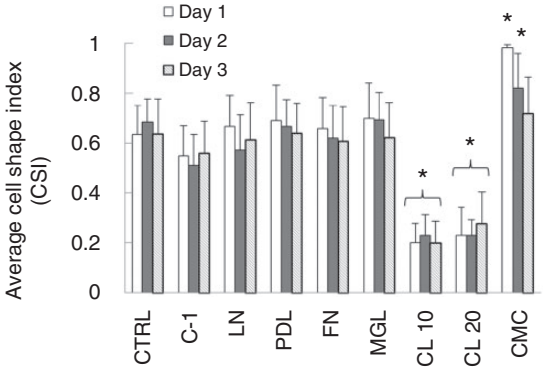

Figure 1. Changes in average CSI of cells cultured on 2D substrates. Measured average CSI of MB-derived Daoy cells cultured on a 2D layer of eight different substrates for 3 days: tissue-culture polystyrene (CTRL), C-1, LN, PDL, FN, MGL, CL10, CL20, and CMC. Values of statistical significance ($p < 0.05$) were measured against control conditions using culture media plates. *Indicates significance with respect to all the other cases. CSI: cell shape index; CTRL: controls; C-1: collagen-1; LN: laminin; PDL: poly-D-lysine; FN: fibronectin; MGL: matrigel; CL10: collagen-laminin 10%; CL20: collagen-laminin 20%; CMC: carboxymethylcellulose.

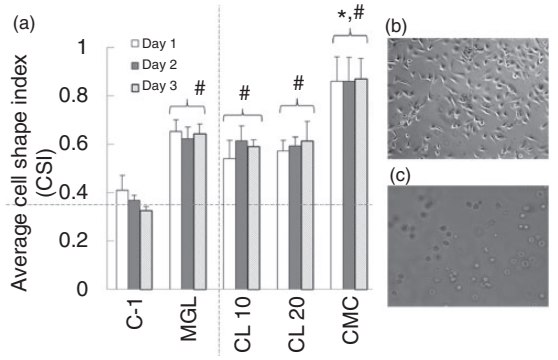

Figure 2. Changes in average CSI of cells within 3D ECM materials. (a) Measured average CSI of MB-derived Daoy cells embedded within 3D ECM microenvironments for t = 3 days: C-1, MGL, CL10, CL20, and CMC. Values of statistical significance were measured against C-1 gels held as controls for these experiments. (b) Representative phase contrast image of cells seeded in C-1 matrices and (c) CMC hydrogels. Mag. = 20 ×. *Indicates significant differences with respect to all the other cases. #Indicates significant difference with respect to C-1. CSI: cell shape index; ECM: extracellular matrix; C-1: collagen-1; MGL: matrigel; CL10: collagen-laminin 10%; CL20: collagen-laminin 20%; CMC: carboxymethylcellulose.

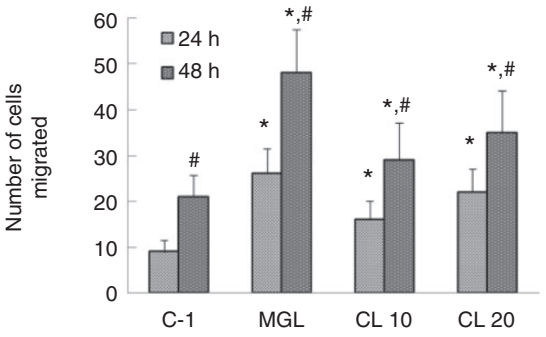

Figure 3. Daoy cell migration within 3D matrices. The average numbers of Daoy cells that migrated through 3D ECM macromolecule gels (C-1, MGL, CL10, and CL20) over 48 h quantified using transwell assays. #Indicates significant differences between 24 and 48 h within each case. *Indicates significant difference with respect to C-1 at respective time points. ECM: extracellular matrix; C-1: collagen-1; MGL: matrigel; CL10: collagen-laminin 10%; CL20: collagen-laminin 20%.

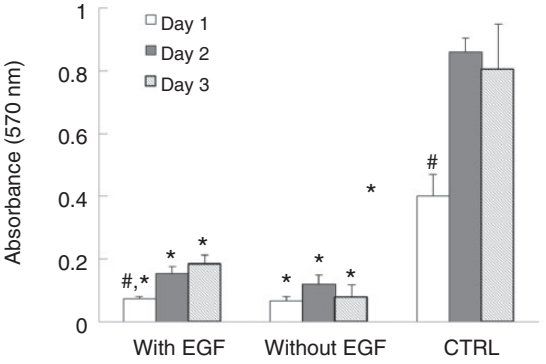

Figure 4. Cell proliferation within CMC hydrogels. An MTT assay demonstrated viability of MB-derived Daoy cells over a span of 3 days in CMC gels with and without exposure to EGF. CTRL consisted of Daoy cells grown on standard tissue-culture dishes. *Indicates significant difference compared to Daoy control on tissue-culture polystyrene at respective time points. #Indicates significant difference compared to day 3 sample within group. CMC: carboxymethylcellulose; EGF: epidermal growth factor; CTRL: controls.

were found when Daoy cells were plated on CL10 and CL20 blends. The cells displayed increased elongation upon both CL10 (0.21 ± 0.01) and CL20 (0.25 ± 0.03) ECM macromolecule formulations, which were significantly different from all other groups but not from each other. Last, cells plated on CMC gels displayed the most rounded morphology with a CSI of 0.84 ± 0.13, which was significantly different from all other groups at 1 and 2 days.

Daoy cells were also grown in 3D hydrogels of varying ECM macromolecule composition. The average measured changes in CSI for Daoy cells grown in the 3D matrices are displayed in Figure 2. No significant differences in CSI values were observed between MGL and CL10 and CL20 blends from day 1 to day 3 (average CSI of 0.587 ± 0.028). The average CSI of cells within C-1 3D gels (average CSI of 0.368 ± 0.042) was significantly less than that of MGL, CL10, CL20, and CMC matrices. The CSI of cells within CMC gels was the highest of those measured (average of 0.863 ± 0.01), indicating that the cells were most rounded. The image in Figure 2(c) illustrates the rounded morphology of Daoy cells in 3D CMC hydrogels in contrast to the more elongated cells on C-1 matrices (Figure 2(b)).

The Daoy-cell chemotactic migration toward EGF was also assessed in the 3D matrices. Figure 3 displays the numbers of cells that migrated through the 3D ECM macromolecule materials after 24 and 48 h. As shown, Daoy cells migrated in largest numbers through ECM macromolecules composed of MGL at both time points, whereas Daoy-cell migration within CL10 and CL20 blends resulted in similar numbers. Cell migration within C-1 gels resulted in the lowest number of cells at both time intervals, which was significantly less than all other culture conditions at each time point. No cells were seen to migrate through CMC gels.

An MTT cell-proliferation assay was used to confirm the viability of cells within CMC gels over 3 days. Cells were seeded onto CMC hydrogels and cultured with or without EGF (Figure 4). Cells exposed to EGF grew continuously on the CMC hydrogels, with MTT absorbance values significantly greater at day 3 in comparison to day 1. Conversely, there was no statistically

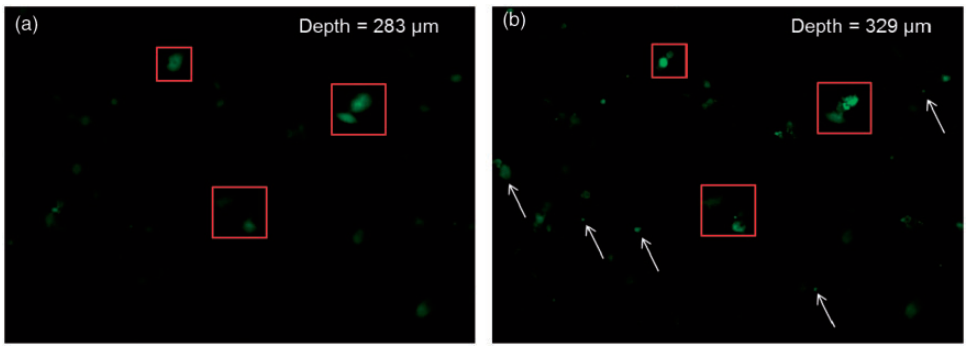

Figure 5. Migration of Daoy cells within CMC hydrogels. (a) A digital section at a depth of 283 μm from a representative CMC hydrogel (550 μm thick); (b) serial Z-stack section at a depth of 329 μm. Specific cells indicated by red boxes are visible in both images. Note the appearance of additional cells on other focal planes (white arrows) in panel (b) while moving through the depth of the gel, indicative of migratory cellular behavior. Scale bar = 50 μm. CMC: carboxymethylcellulose.

significant difference in absorbance measurements between days 1 and 3 for cells not exposed to EGF. CTRL on tissue-culture polystyrene displayed the highest level of cell growth.

Spectral analysis of 3D CMC hydrogels was performed to measure the average penetration depth within the matrix at different time intervals. Figure 5 shows the cells in different planes within a representative CMC hydrogel approximately 550 μm in thickness.

Immunocytochemistry was carried out to examine the different expression levels of the $\alpha_v\beta_3$ surface integrin believed to be important for Daoy-cell migration upon ECM macromolecules (Figure 6(a) to (e)). Figure 6(f) shows the average $\alpha_v\beta_3$ expression for cells plated on MGL, C-1, CMC, LN, and CTRL. MGL is seen to promote the highest level of integrin expression, followed by C-1. CMC and LN exhibit similar levels of integrin expression, much lower than that of the other matrix macromolecules.

Discussion

The migration of cells from pediatric brain tumors has been largely understudied despite their high-tumor metastatic potential and aggressive invasion into healthy brain.[14] While interactions between cells and ECM macromolecules have been widely investigated, the migrational behavior of Daoy cells within synthetic hydrogels is unknown.

This work examined the use of a novel CMC biomaterial for *in vitro* study of Daoy motility and chemotaxis. Although numerous ECM macromolecules have been used in the last decade to examine cell migration *in vitro*, it is well known that many of the proteins used can themselves stimulate migration via interactions with cell-surface receptors.[44,45] Such ECM macromolecule-induced migration limits the usefulness of *in vitro* testing of anti-migratory therapies and pharmacological agents and has contributed to diminished interest in anti-migratory targets in MB.

CMC is a negatively charged, largely inert biomaterial known for its application in dermal fillers and for oral drug-delivery vehicles.[46–48] CMC was chosen since it was thought to provide an anchorage-free microenvironment similar to that experienced by Daoy cells *in vivo*. Also, the 3D anionic CMC matrix is analogous to that provided by the negatively charged proteoglycans abundant in brain tissue.[49,50] Moreover, CMC does not contain soluble growth factors or adhesive ligands present in the native MB environment, thereby enabling more controlled testing of MB chemotactic pathways and cell responses.

The first set of experiments was conducted to quantitatively describe how Daoy-cell shape is affected by seven of the most commonly used substrates in studies of CNS-derived cells: C-1, LN, CL10 and CL20 blends, MGL, FN, and PDL. As illustrated in Figures 1 and 2, the CSI was used as a measure of the roundness of Daoy cells on 2D and within 3D matrix environments. This was employed because cells with more elongated morphological characteristics are believed to possess a readiness to migrate, while cells with a more rounded shape are considered to be less predisposed to motility.[14,51,52] However, such elongated morphology in our case would equate to ECM macromolecule-driven crawling or haptotaxis, which is integrin mediated. A "haptotaxis-neutral" biomaterial was purposely selected in order to develop an *in vitro* platform with which to examine chemotactic behaviors. Specifically, it was of interest to determine how such cell chemotaxis can be directed by external concentration profiles generated via pharmacological treatment and/or therapies. As CMC showed the most promise of maintaining a rounded cell shape, the next set of experiments examined growth factor-induced chemotaxis

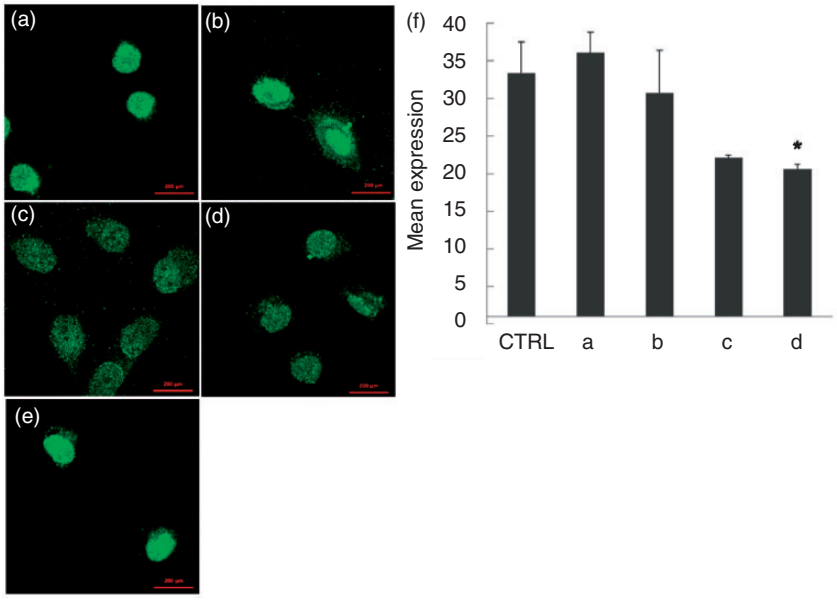

Figure 6. Comparative mean intensity of integrin $\alpha_v\beta_3$ expression measured from cells plated on different substrates. ICC of $\alpha_v\beta_3$ (green) on cells adhered upon (a) MGL; (b) C-1; (c) CMC hydrogel; (d) LN; and (e) tissue-culture polystyrene (CTRL). (f) Average normalized fluorescence expression measured from cell samples (n = 4). *Indicates significant difference with respect to (a). MGL: matrigel; C-1: collagen-1; CMC: carboxymethylcellulose; LN: laminin; CTRL: controls.

(using EGF) within a 3D microenvironment created using CMC.

Results of transwell migration assays in Figure 3 illustrated that virtually all of the other ECM macromolecules tested were more conducive to EGF-induced migration, as zero cells were seen to migrate through the thick gel generated using CMC. However, closer inspection revealed that Daoy cells did indeed survive and migrate within CMC gels for several days, with and without EGF stimulation, as seen in Figure 4. Data in Figure 5 demonstrated that Daoy cells were not measured in transwell assays because the cells migrated distances less than the thickness of the CMC gel used in conjunction with the migration membrane. This result was encouraging, as Daoy cells *in vivo* are not expected to migrate in large numbers over short times.

The mechanism of Daoy cell interaction with the CMC gels was then examined by analyzing the expression of $\alpha_v\beta_3$ integrin, which is known to be critical to MB mobility *in vitro* and *in vivo*.[44,53,54] As expected, MGL exhibited the highest integrin expression, given its rich environment of growth factors, followed by C-1 and CTRL. However, Daoy cells exhibited the same level of $\alpha_v\beta_3$ expression upon CMC surfaces as they did upon surfaces of LN, which is ubiquitous in the study of CNS-derived cells because of the protein's prominence in the brain.[44,55–57] Similar levels of $\alpha_v\beta_3$ expression between these two matrices were surprising, as it suggests that Daoy cells engage CMC gels in a manner similar to the highly studied LN. Nevertheless, previous work examining spontaneous metastasis of breast tumors to bone has reported that tumor-specific $\alpha_v\beta_3$ integrins mediate chemotactic migration of mammary carcinoma cells in response to bone-derived soluble factors.[58] $\alpha_v\beta_3$ integrins may play a similar role in MB metastasis. Future studies with neutralizing antibodies to $\alpha_v\beta_3$ could help elucidate the role of this specific integrin in MB-derived Daoy-cell chemotaxis.

Conclusions

Taken together, these findings demonstrate that CMC hydrogels allow for minimal spreading and associated haptotactic migration by Daoy cells, which are conducive to mechanistic studies of cellular chemotactic behavior. Detailed knowledge of cell–ECM interactions is important for understanding the mechanisms by which cells are regulated by microenvironmental cues. As such, this CMC hydrogel system may serve as an effective tool to gain insight into specific tumor-cell metastatic processes mediated by soluble signaling factors.

Conflict of interest

None declared.

Funding

This work was supported by the National Science Foundation (CAREER CBET 0747968 and DMR 1207480 to SBN and

CBET 0939511 to MV) and National Institute of Health (1454CA143798-01).

References

1. Berrier AL and Yamada KM. Cell-matrix adhesion. *J Cell Physiol* 2007; 213: 565–573.
2. Lu P, Weaver VM and Werb Z. The extracellular matrix: a dynamic niche in cancer progression. *J Cell Biol* 2012; 196: 395–406.
3. Zaman MH, Trapani LM, Sieminski AL, et al. Migration of tumor cells in 3D matrices is governed by matrix stiffness along with cell-matrix adhesion and proteolysis. *Proc Natl Acad Sci USA* 2006; 103: 10889–10894.
4. Egeblad M, Rasch MG and Weaver VM. Dynamic interplay between the collagen scaffold and tumor evolution. *Curr Opin Cell Biol* 2010; 22: 697–706.
5. Ma HL, Jiang Q, Han S, et al. Multicellular tumor spheroids as an in vivo-like tumor model for three-dimensional imaging of chemotherapeutic and nano material cellular penetration. *Mol Imag* 2012; 11: 487–498.
6. Bignon M, Pichol-Thievend C, Hardouin J, et al. Lysyl oxidase-like protein-2 regulates sprouting angiogenesis and type IV collagen assembly in the endothelial basement membrane. *Blood* 2011; 118: 3979–3989.
7. Davis GE and Senger DR. Endothelial extracellular matrix: biosynthesis, remodeling, and functions during vascular morphogenesis and neovessel stabilization. *Circul Res* 2005; 97: 1093–1107.
8. Pakulska MM, Ballios BG and Shoichet MS. Injectable hydrogels for central nervous system therapy. *Biomed Mater* 2012; 7: 024101.
9. Hashizume H, Baluk P, Morikawa S, et al. Openings between defective endothelial cells explain tumor vessel leakiness. *Am J Pathol* 2000; 156: 1363–1380.
10. Hewitt RE, Powe DG, Morrell K, et al. Laminin and collagen IV subunit distribution in normal and neoplastic tissues of colorectum and breast. *Br J Cancer* 1997; 75: 221–229.
11. Egeblad M, Nakasone ES and Werb Z. Tumors as organs: complex tissues that interface with the entire organism. *Dev Cell* 2010; 18: 884–901.
12. Ruoslahti E. Specialization of tumour vasculature. *Nat Rev Cancer* 2002; 2: 83–90.
13. Bosman FT and Stamenkovic I. Functional structure and composition of the extracellular matrix. *J Pathol* 2003; 200: 423–428.
14. Richard A, Able J, Dudu V, et al. *Migration and invasion of brain tumor*. Croatia: InTech, 2011, p.498.
15. Baker BM and Chen CS. Deconstructing the third dimension: how 3D culture microenvironments alter cellular cues. *J Cell Sci* 2012; 125: 3015–3024.
16. Carragher NO. Profiling distinct mechanisms of tumour invasion for drug discovery: imaging adhesion, signalling and matrix turnover. *Clin Exp Metastas* 2009; 26: 381–397.
17. Nyga A, Cheema U and Loizidou M. 3D tumour models: novel in vitro approaches to cancer studies. *J Cell Commun Signal* 2011; 5: 239–248.
18. Simao D, Costa I, Serra M, et al. Towards human central nervous system in vitro models for preclinical research: strategies for 3D neural cell culture. *BMC Proc* 2011; 5(Suppl 8): P53.
19. Smalley KS, Lioni M and Herlyn M. Life isn't flat: taking cancer biology to the next dimension. *In Vitro Cell Dev Biol Animal* 2006; 42: 242–247.
20. Ljubimova JY, Fujita M, Khazenzon NM, et al. Changes in laminin isoforms associated with brain tumor invasion and angiogenesis. *Front Biosci: J Virtual Lib* 2006; 11: 81–88.
21. Friedl P and Brocker EB. The biology of cell locomotion within three-dimensional extracellular matrix. *Cell Mol Life Sci CMLS* 2000; 57: 41–64.
22. Cho Y and Borgens RB. Polymer and nano-technology applications for repair and reconstruction of the central nervous system. *Exp Neurol* 2012; 233: 126–144.
23. Kasoju N and Bora U. Silk fibroin in tissue engineering. *Adv Healthcare Mater* 2012; 1: 393–412.
24. Lee SJ and Atala A. Scaffold technologies for controlling cell behavior in tissue engineering. *Biomed Mater* 2013; 8: 010201.
25. Ozeki T, Kaneko D, Hashizawa K, et al. Combination therapy of surgical tumor resection with implantation of a hydrogel containing camptothecin-loaded poly(lactic-co-glycolic acid) microspheres in a C6 rat glioma model. *Biol Pharm Bull* 2012; 35: 545–550.
26. Woerly S. Restorative surgery of the central nervous system by means of tissue engineering using NeuroGel implants. *Neurosurg Rev* 2000; 23: 59–77. (discussion 8–9).
27. Wolf K and Friedl P. Extracellular matrix determinants of proteolytic and non-proteolytic cell migration. *Trends Cell Biol* 2011; 21: 736–744.
28. Ulrich TA, de Juan Pardo EM and Kumar S. The mechanical rigidity of the extracellular matrix regulates the structure, motility, and proliferation of glioma cells. *Cancer Res* 2009; 69: 4167–4174.
29. Whittemore SR, Zhang YP, Shields CB, et al. Optimizing stem cell grafting into the CNS. *Methods Mol Biol* 2008; 438: 375–382.
30. Even-Ram S and Yamada KM. Cell migration in 3D matrix. *Curr Opin Cell Biol* 2005; 17: 524–532.
31. Kim Y, Stolarska MA and Othmer HG. The role of the microenvironment in tumor growth and invasion. *Prog Biophys Mol Biol* 2011; 106: 353–379.
32. Liotta LA. Tumor invasion and metastases—role of the extracellular matrix: Rhoads Memorial Award lecture. *Cancer Res* 1986; 46: 1–7.
33. Pupa SM, Menard S, Forti S, et al. New insights into the role of extracellular matrix during tumor onset and progression. *J Cell Physiol* 2002; 192: 259–267.
34. Lee MR and Jeon TJ. Cell migration: regulation of cytoskeleton by Rap1 in *Dictyostelium discoideum*. *J Microbiol* 2012; 50: 555–561.
35. Servais C and Erez N. From sentinel cells to inflammatory culprits: cancer-associated fibroblasts in tumour-related inflammation. *J Pathol* 2013; 229: 198–207.
36. Decaestecker C, Debeir O, Van Ham P, et al. Can anti-migratory drugs be screened in vitro? A review of 2D and 3D assays for the quantitative analysis of cell migration. *Med Res Rev* 2007; 27: 149–176.

37. Millerot-Serrurot E, Guilbert M, Fourre N, et al. 3D collagen type I matrix inhibits the antimigratory effect of doxorubicin. *Cancer Cell Int* 2010; 10: 26.
38. Reza AT and Nicoll SB. Characterization of novel photocrosslinked carboxymethylcellulose hydrogels for encapsulation of nucleus pulposus cells. *Acta Biomater* 2010; 6: 179–186.
39. Gupta MS, Cooper ES and Nicoll SB. Transforming growth factor-beta 3 stimulates cartilage matrix elaboration by human marrow-derived stromal cells encapsulated in photocrosslinked carboxymethylcellulose hydrogels: potential for nucleus pulposus replacement. *Tissue Eng Part A* 2011; 17: 2903–2910.
40. Dudu V, Rotari V and Vazquez M. Targeted extracellular nanoparticles enable intracellular detection of activated epidermal growth factor receptor in living brain cancer cells. *Nanomed Nanotechnol Biol Med* 2011; 7: 896–903.
41. Kong Q, Majeska RJ and Vazquez M. Migration of connective tissue-derived cells is mediated by ultra-low concentration gradient fields of EGF. *Exp Cell Res* 2011; 317: 1491–1502.
42. Shen JY, Chan-Park MB, He B, et al. Three-dimensional microchannels in biodegradable polymeric films for control orientation and phenotype of vascular smooth muscle cells. *Tissue Eng* 2006; 12: 2229–2240.
43. Dudu V, Able Jr RA, Rotari V, et al. Role of epidermal growth factor-triggered PI3K/Akt signaling in the migration of medulloblastoma-derived cells. *Cell Mol Bioeng* 2012; 5: 402–413.
44. Pilorget A, Berthet V, Luis J, et al. Medulloblastoma cell invasion is inhibited by green tea (−)epigallocatechin-3-gallate. *J Cell Biochem* 2003; 90: 745–755.
45. Friedl P, Zanker KS and Brocker EB. Cell migration strategies in 3-D extracellular matrix: differences in morphology, cell matrix interactions, and integrin function. *Microsc Res Tech* 1998; 43: 369–378.
46. Falcone SJ, Doerfler AM and Berg RA. Novel synthetic dermal fillers based on sodium carboxymethylcellulose: comparison with crosslinked hyaluronic acid-based dermal fillers. *Dermatol Surg: Off Publ Am Soc Dermatol Surg [et al.]* 2007; 33(Suppl 2): S136–S143. (discussion S43).
47. Leonardis M, Palange A, Dornelles RF, et al. Use of cross-linked carboxymethyl cellulose for soft-tissue augmentation: preliminary clinical studies. *Clin Interv Aging* 2010; 5: 317–322.
48. Dastoor SF, Misch CE and Wang HL. Dermal fillers for facial soft tissue augmentation. *J Oral Implantol* 2007; 33: 191–204.
49. Ruoslahti E. Brain extracellular matrix. *Glycobiology* 1996; 6: 489–492.
50. Zimmermann DR and Dours-Zimmermann MT. Extracellular matrix of the central nervous system: from neglect to challenge. *Histochem Cell Biol* 2008; 130: 635–653.
51. Giese A, Loo MA, Tran N, et al. Dichotomy of astrocytoma migration and proliferation. *Int J Cancer* 1996; 67: 275–282.
52. Hatzikirou H, Basanta D, Simon M, et al. 'Go or grow': the key to the emergence of invasion in tumour progression? *Math Med Biol: J IMA* 2012; 29: 49–65.
53. Kishima H, Shimizu K, Tamura K, et al. Monoclonal antibody ONS-M21 recognizes integrin alpha3 in gliomas and medulloblastomas. *Br J Cancer* 1999; 79: 333–339.
54. MacDonald TJ and Ladisch S. Antisense to integrin alpha v inhibits growth and induces apoptosis in medulloblastoma cells. *Anticancer Res* 2001; 21: 3785–3791.
55. Bruckner G, Grosche J, Hartlage-Rubsamen M, et al. Region and lamina-specific distribution of extracellular matrix proteoglycans, hyaluronan and tenascin-R in the mouse hippocampal formation. *J Chem Neuroanaty* 2003; 26: 37–50.
56. Giordana MT, Germano I, Giaccone G, et al. The distribution of laminin in human brain tumors: an immunohistochemical study. *Acta Neuropathol* 1985; 67: 51–57.
57. Jucker M, Tian M and Ingram DK. Laminins in the adult and aged brain. *Mol Chem Neuropathol* 1996; 28: 209–218.
58. Sloan EK, Pouliot N, Stanley KL, et al. Tumor-specific expression of alphavbeta3 integrin promotes spontaneous metastasis of breast cancer to bone. *Breast Cancer Res* 2006; 8: R20.